

## Article

# Advancing Erosion Control Analysis: A Comparative Study of Terrestrial Laser Scanning (TLS) and Robotic Total Station Techniques for Sediment Barrier Retention Measurement

Junshan Liu <sup>\*</sup>, Robert A. Bugg and Cort W. Fisher 

McWhorter School of Building Science, Auburn University, Auburn, AL 36849, USA;  
rab0018@auburn.edu (R.A.B.); cwf0002@auburn.edu (C.W.F.)

\* Correspondence: liujuns@auburn.edu; Tel.: +1-334-844-5387

**Abstract:** Sediment Barriers (SBs) are crucial for effective erosion control, and understanding their capacities and limitations is essential for environmental protection. This study compares the accuracy and effectiveness of Terrestrial Laser Scanning (TLS) and Robotic Total Station (RTS) techniques for quantifying sediment retention in SBs. To achieve this, erosion tests were conducted in a full-scale testing apparatus with TLS and RTS methods to collect morphological data of sediment retention surfaces before and after each experiment. The acquired datasets were processed and integrated into a Building Information Modeling (BIM) platform to create Digital Elevation Models (DEMs). These were then used to calculate the volume of accumulated sediment upstream of the SB system. The results indicated that TLS and RTS techniques could effectively measure sediment retention in a full-scale testing environment. However, TLS proved to be more accurate, exhibiting a standard deviation of 0.41 ft<sup>3</sup> in contrast to 1.94 ft<sup>3</sup> for RTS and more efficient, requiring approximately 15% to 50% less time per test than RTS. The main conclusions of this study highlight the benefits of using TLS over RTS for sediment retention measurement and provide valuable insights for improving erosion control strategies and sediment barrier design.



**Citation:** Liu, J.; Bugg, R.A.; Fisher, C.W. Advancing Erosion Control Analysis: A Comparative Study of Terrestrial Laser Scanning (TLS) and Robotic Total Station Techniques for Sediment Barrier Retention Measurement. *Geomatics* **2023**, *3*, 345–363. <https://doi.org/10.3390/geomatics3020019>

Academic Editors: Jin Liu, Shengyuan Song, Huilin Le and Yunjian Li

Received: 30 March 2023

Revised: 16 April 2023

Accepted: 24 April 2023

Published: 26 April 2023



**Copyright:** © 2023 by the authors. Licensee MDPI, Basel, Switzerland. This article is an open access article distributed under the terms and conditions of the Creative Commons Attribution (CC BY) license (<https://creativecommons.org/licenses/by/4.0/>).

**Keywords:** erosion control; laser scanning; LiDAR; reality capture; sediment retention; silt fence

## 1. Introduction

Erosion is a common problem on construction job sites worldwide [1]. Whether it is the construction of buildings or roads, there is a need to control sediment runoff from project sites. When job sites are cleared of natural vegetation, conditions for erosion are enhanced. Sediment transport increases when erosion rates are accelerated by rainfall landing on unprotected and unvegetated areas disturbed during earthwork [2]. Sediment eroded from a construction site can end up on neighboring properties, streets, sewer systems, creeks, and rivers. The effects of sediment-laden effluent emanating from land-disturbing activities and the need to implement effective stormwater pollution prevention measures to protect the waterways were recognized by the Clean Water Act of 1972 and the Water Quality Act of 1987 of the US [3]. A construction company that does not adhere to the requirements of the Clean Water Act or other related regulations can incur significant fines. There are several erosion and sediment control systems commonly employed. These include diversion swales, erosion control blankets, sediment basins, vegetation barriers, and sediment barriers (SBs) [2,4]. SBs are the most commonly used option in the construction industry in the US [4,5].

An SB is a temporary structure typically built around the edge of construction sites or other locations with bare soil [6]. As erosion occurs, the SB's primary function is to slow the water flow and create a temporary dam while allowing water to filter through. In an optimal scenario, this “pooling” effect upstream of the barrier allows time for most of the sediment to settle while a minimal amount makes it downstream. Unfortunately, factors

such as its structural integrity and sediment build-up on the fabric can cause the SB to fail or break down. Furthermore, the flow-through capacity of the fencing material has the potential to degrade over time as pores in the material become clogged with sediment [2]. Therefore, testing SB systems and knowing their limitations regarding sediment retention is an important subject but a relatively new area of research in this field. Calculating how much sediment is retained by a certain type of sediment barrier is a technique that benefits the manufacturers of these products, designers of erosion control systems, and end-users. These calculations can be in the form of volumetric data based on before and after tests. However, until recently, most SB testing was done through small-scale testing methodologies that have failed to address realistic stormwater runoff volumes, flow rates, or sediment loadings that in-field SB installations will most likely intercept throughout their life cycle [7].

A full-scale SB testing apparatus was recently established at the Auburn University-Erosion and Sediment Control Testing Facility (AU-ESCTF) in Auburn, Alabama, USA. This apparatus has allowed for new research and testing as it can replicate a 2-year, 24-hour storm event in a realistic, controlled setting [8]. Most importantly, with this apparatus, the effectiveness of different sediment barriers can be more accurately tested [5]. In a full-scale setting, such as the apparatus at AU-ESCTF, measuring sediment retention had only been performed with a Total Station (TS) surveying device [5] before this research. This TS technique has some significant issues, such as lack of precision, human errors, and disturbance of the sediment surface. Having two people recording hundreds of recordings manually also makes the TS technique very labor-intensive and subject to discrepancies in data [9]. This research aims to investigate the implementation of advanced Reality Capture (RC) techniques, including Terrestrial Laser Scanning (TLS) and Robotic Total Station (RTS) surveys, to quantify sediment retention and develop a more accurate and effective method to measure sediment deposits.

## 2. Literature Review

### 2.1. Sediment Barriers and Testing

There are three types of SB practices: manufactured silt fence systems, sediment retention barriers (SRBs), and manufactured sediment barrier products [2]. Manufactured silt fence systems are the most commonly used on construction sites today because of several factors, including longevity, durability, portability, and ease of installation and maintenance [10–12]. They usually consist of wooden or metal posts and fabric ready for installation. All that must be done on job sites is the trenching to get them set up. An SRB combines two parallel silt fence instalments with bales of hay put in between [3]. To install the manufactured sediment barrier products, wooden posts are required to hold the SRB in place [2].

Most of the published literature on SB has focused on testing geotextile silt fences on small testing apparatus. Whitman et al. [3] compared flow rates, sediment retention capabilities, and water quality impacts on geotextile silt fences with woven-type and nonwoven-type fabrics. The results of the study showed that nonwoven textiles outperformed woven. Another study was conducted on a tilting testbed with simulated rainfall using these two different fabrics, proving that nonwoven textiles outperformed woven textiles as well [13]. Keener et al. [14] researched flow rates through compost filter socks versus silt fences with 120 test runs to determine the flow through capacity and filtration efficiencies. Their findings included ponding occurring more rapidly behind the silt fence, and silt socks are more stable than silt fences at lower flow rates.

Other research experiments examined different configurations of SBs and their installation techniques. For example, one study evaluated the performance of 8 alternative configurations of the Alabama Department of Transportation (ALDOT) standard wire-backed fence [5], which revealed that (1) most SB structural failure was due to T-post deflection; (2) no improvement in water quality downstream of the installation was observed; and (3) the majority of sediment introduced was retained upstream of the in-

stallation. As a result, various recommendations were presented by the research team to ALDOT for improving the structural ability of the SBs, including a lower fence, a decrease in post spacing and heavier T-posts.

Research has also been done on tiebacks with SBs using an intermediate-scale laboratory model [15]. A tieback is a short extension at either end of an SB that creates a “j-hook”. The research showed that a well-designed SB fence with tiebacks could remove up to 90% of solids transported by runoff water in a highway setting [15].

## 2.2. Quantifying Sediment Retention of Sediment Barriers

All these experimental studies on SBs mentioned above required the quantification of sediment retention. However, very limited published literature focused on technology and techniques for measuring sediment deposits. For example, Zimmie and Kamalzare [16] proposed a method to determine the quantity and rate of small-scale erosion with adequate precision. They used a Kinect sensor part of a Microsoft gaming system to look at a model with different elevations. The elevations for the model were created in a centrifuge and measured at different intervals. Another study looked at photogrammetry technology to measure the surface roughness of samples in a small laboratory setting [17]. An apparatus was created with turbidity sensors on the downstream and upstream ends of the flume. Samples were put in an apparatus, and photos were taken after each test. The results of this study showed that the stereophotogrammetry computational program could accurately measure the surface roughness of the soil samples.

## 2.3. Methods of Measuring Erosion Rates

Due to the lack of publications exclusively on the quantification of sediment retention of SBs, the literature review of this study was expanded to the studies of methodology to evaluate erosion rates and sediment yield.

Multi-temporal high-resolution Digital Elevation Model (DEM) analysis has been widely used to quantify morphology surfaces [18], such as eroded topo-surface, with remote sensing techniques such as Terrestrial Laser Scanning (TLS) [19–21]. DEM is a data file containing the elevation of the terrain in a specified area [9]. TLS uses LiDAR (Light Detection And Ranging) technology to create high-density point clouds of the area showing three-dimensional topography by combining laser-based distance measurements with precise orientation [22]. TLS data acquisition has led to multi-temporal DEMs that archive the same region as a series of time slices [23,24]. The derived DEMs of this region can then be analyzed sequentially to obtain DEMs of difference (DoDs), which reveal not only the horizontal but also the accurate vertical and volumetric pattern of topographic changes. Such assessments of geomorphic changes based on DoDs provide information on landscape morphology and evolution. In addition, it enables a detailed study of the spatial and temporal patterns in surface erosion and deposition [25]. Compared to conventional survey techniques, TLS paired with DEM was proven more effective in topography mapping and detecting changes in terrain [26–28]. A primary advantage of TLS is that it can detect the precise surface position and shape changes with up to one millimeter (mm) resolution [29]. Comparing TLS scans, surface elevation changes could be quantified at an accuracy level better than 1 mm and a mean level of change detection less than 2.2 mm [30]. Another advantage of TLS is that it can provide spatial information without disturbing the observed surface [31]. The few drawbacks of using TLS for monitoring erosion rates include its limitations to small plots only [19] and high equipment cost [24].

Total Station (TS) survey can also effectively show how the shape of the topographic surface changes over time from erosion or deposition by accurately measuring the locations of specific points [9,18,22]. However, a TS can only capture one point on the surface at a time. Therefore, the TS survey requires a systematic method to record enough points to cover a particular area. A common TS survey approach is capturing points on a path at a fixed grid interval, as shown in Figure 1. The smaller the grid intervals, the more detailed the information will be recorded [9]. Nevertheless, it also means more points to capture,

and a longer surveying time is needed. Therefore, one of the most significant disadvantages of the TS technique is the long surveying time [9]. Also, TS data can be coarse, and lacks point density, which is needed to accurately model surface details. Furthermore, unlike the non-contact TLS technique, TS surveys with a prism rod can disturb the topography [22,23].

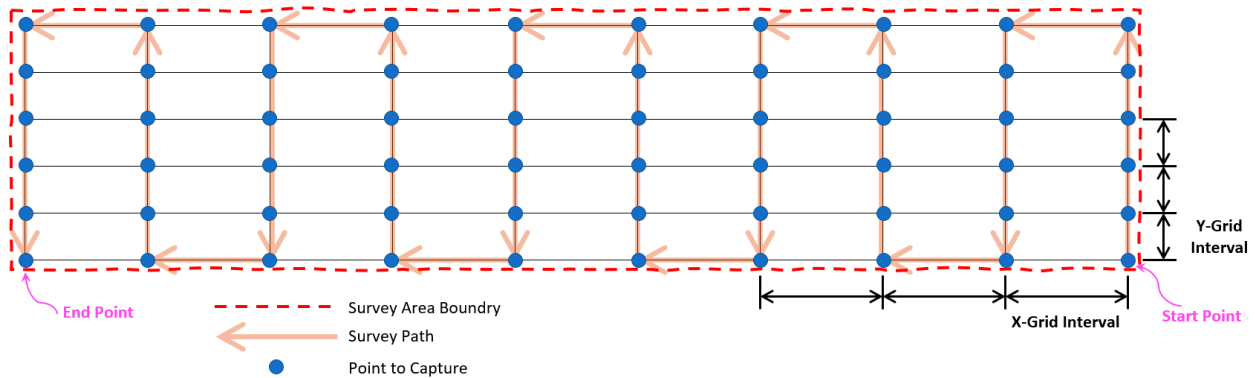


Figure 1. A Total Station (TS) survey approach to capture points of a topographic surface.

### 3. Materials and Methods

The methodology of this research includes Stage-1 for field tests and data collection and Stage-2 for data processing and result analysis. During Stage-1, three tests were run in a full-scale apparatus that simulated an erosion event after rainfall. Then both TLS and RTS techniques were used to capture the surface information of the sediment retention area. In Stage-2, the captured surface data was used to create Digital Elevation Models (DEMs) for calculating the volume of the sediment deposit of each test. Figure 2 illustrates a detailed workflow and related materials used in the different steps of this research study.

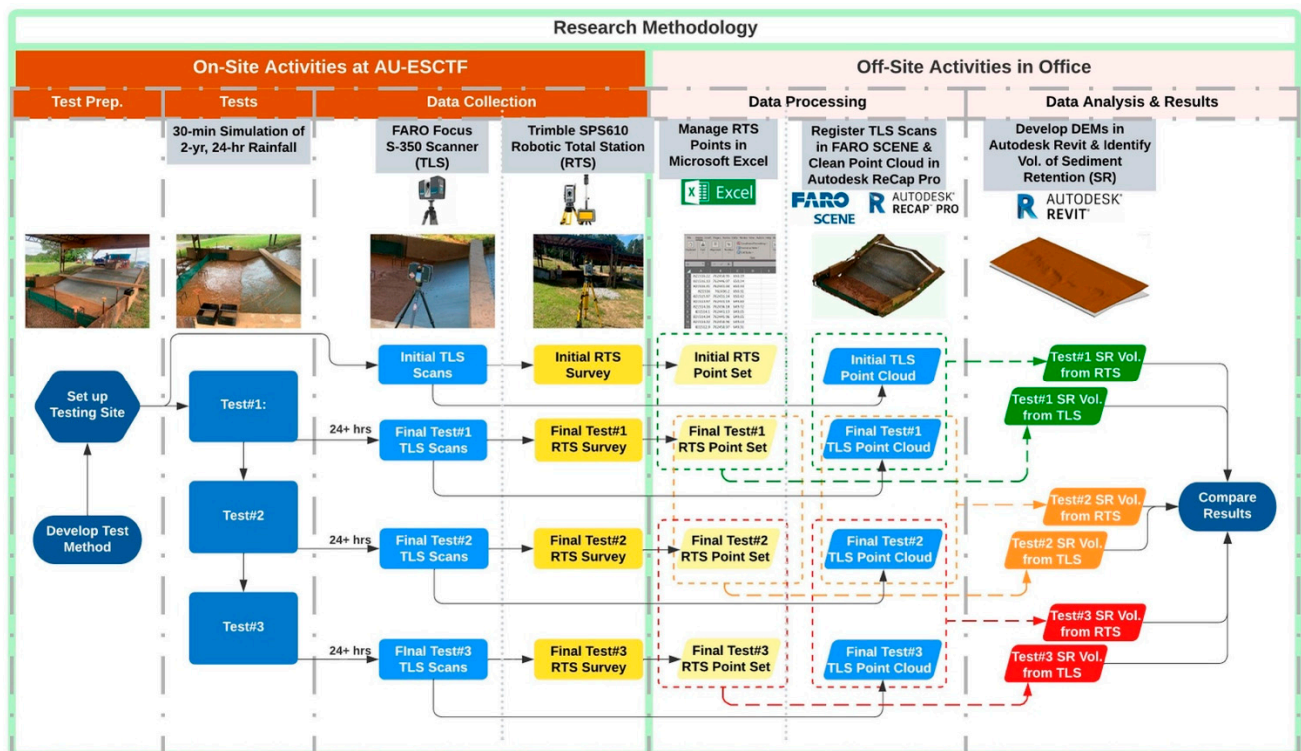


Figure 2. A detailed workflow and related materials used for this research study.

### 3.1. Experimental Apparatus and Equipment

Until recently, the standards for testing sediment barriers had been limited to small experimental settings. However, with the growing experimentation and research on erosion control devices, more suggestions for different types of testing are being examined. A response to ALDOT's (Alabama Department of Transportation) interest in this experimentation has led to a full-scale testing facility being built at the AU-ESCTF [2]. This facility was designed to replicate field-like conditions. Standards used at this facility for testing SBs consist of structural integrity, erosion and sediment deposition, ponding and discharge measurements, and turbidity and total suspended solids [32].

In preparation for the tests for this research study, a full-scale testing apparatus (Figure 3a) was established at Station D of AU-ESCTF. The significant elements of this apparatus included a fill slope where erosion was expected to occur, a rainfall simulator, a silt fence installation zone, and an area to collect erosion sediment (Figure 3b). The rainfall simulator consisted of a water tank (Figure 3c), a water flow gauge (Figure 3d), and a mixing trough (Figure 3e). The ground of the collection area was leveled before the initial test. The silt fence was installed with a tieback at either end (Figure 3b). For the tests of this research, the field testing method was designed based on Whitman et al. [7], aiming to simulate the average 30-min peak flow resulting from a 2-year, 24-h rainstorm event in central Alabama, with water originating from a 1/2 acre (0.20 ha) drainage basin, thus ensuring the accuracy and relevance of the tests under realistic conditions.



(a)



(b)



(c)

Figure 3. Cont.



**Figure 3.** A full-scale erosion testing apparatus for this research study: (a) A full-scale testing apparatus; (b) Sediment collection area and silt fence; (c) Water tank connected to a pump; (d) Water flow gauge; (e) Soil and water mixing trough.

This study used two pieces of Reality Capture (RC) equipment to capture data for measuring the volume of sediment retention: a FARO Focus S-350 Laser Scanner (FARO S-350) and a Trimble SPS610 5" Robotic Total Station (Trimble SPS610).

The FARO S-350 is one of the most commonly used TLS scanners in the Architecture, Engineering and Construction (AEC) industry [33]. This scanner was used to capture the morphology of the testing surface.

The Trimble SPS610 is a Robotic Total Station (RTS) [34]. An RTS is a TS that allows remote operation. This means it only requires one operator and can perform more calculations and inspections in less time than a traditional TS [35]. This RTS captured point elevations on the testing surface after completing the TLS scanning.

### 3.2. Experimental Procedure

The first step in preparing the apparatus for testing was to get the soil ready. A stockpile of soil native to the state of Alabama and classified as loam (46.9% sand, 28.1% silt, 25.0% clay) according to the USDA was prepared on-site [32]. Thirty buckets were filled with the soil (each weighing 32 lbs./14.5 kg) and stacked into the bed of a pick-up truck that was backed to the trough area at the top of the slope, as seen in Figure 3a. Next, the water supply was set up and calibrated. A gasoline-powered pump was used to pump water from a holding pond to the water storage tank at the top of the testing unit (Figure 3c). Once the water in the tank reached a certain level, the water flowed through a discharge weir into the mixing trough at a calibrated rate. The flow was controlled by valves and monitored by a gauge mounted to the side of the water tank, as shown in Figure 3d. Water would then flow from the mixing trough (Figure 3e) onto the test slope via a discharge channel, which flowed evenly down towards the test area.

All three tests were run during the afternoon on three different days. This consistent afternoon schedule minimized the impact of external factors, such as daylight and temperature, on the results, enhancing the reliability of the findings. Once everything was in place and ready to go, the pump started, and water was pumped into the tank. When the correct water flow was achieved at 0.22 cfs. (6.23 L/s), a stopwatch was started, and 30 buckets (960 lbs./435 kgs) of soil were manually and continually poured into the trough at one bucket every minute to mix with the water (Figure 4a). The mixture flowed down the slope at an evenly distributed flow for 30 min (Figure 4b). Figure 4c illustrates the water and soil mixture accumulated in the testing area. Once the test was complete and the last bucket of soil was applied, the pump was turned off, and the testing area was left to drain. The area would be left to sit for at least 24 h for dewatering before measurements were

taken, ensuring accurate sediment retention quantification. Figure 4d shows the drained testing area.



**Figure 4.** Erosion test in the full-scale apparatus: (a) Soil and water mixed in the trough at a constant rate; (b) Flow of sediment with water; (c) Mixture of water and soil accumulated in the testing area; (d) Drained testing area before measurements were taken.

### 3.3. Data Collection

TLS and RTS techniques were used to capture the topography of the sediment retention in the testing area before the initial test and then 24 h after each subsequent test.

#### 3.3.1. TLS Scanning

For the TLS scanning, four locations were chosen to set up the FARO S-350 laser scanner around the perimeter of the testing area to ensure that sufficient morphological information was collected (Figure 5a). Each of these four scan locations was marked with a survey-nail wrapped with a piece of red tape (Figure 5b), which ensured that the TLS scans would take place at the same locations for all the tests. The FARO S-350's scanning resolution chosen for this research was 1/4 with a quality setting of 3X. This configuration allowed the scanner to capture up to 43.7 million points in 6 min with a point cloud density of 6.1 mm at a 10 m distance. The scanner's color mode (non-HDR) was also turned on to record panoramic photos that were later used for colorizing the point clouds. On average, one TLS scan took about twelve minutes, including scan station setup (6 min) and scanning and capturing panoramic photos (6 min).

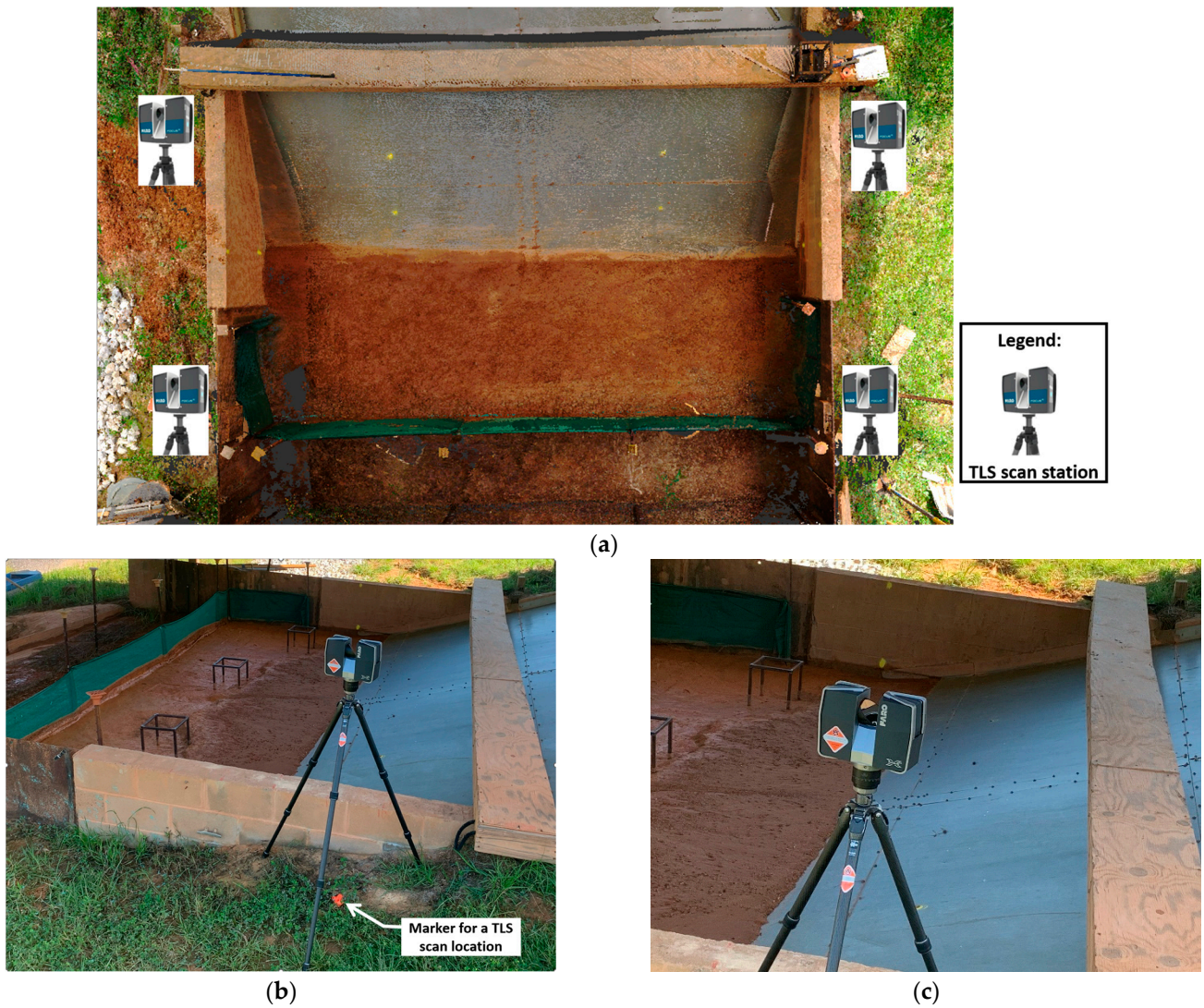


**Figure 5.** TLS scanning of the testing area: (a) The 4 locations where the FARO S-350 scanner was set up to scan the testing area; (b) A TLS scan location was marked; (c) The FARO S-350 scanned the testing area after the first test.

An initial set of four TLS scans of the testing area was captured before any tests took place, with the area being level and clean. A set of four scans then took place from the same locations 24 h after each subsequent test (Figure 5c). The total time spent on TLS for each test was approximately one hour.

### 3.3.2. RTS Survey

Using three pre-established control points, the Trimble SPS610 5" RTS was set up next to the apparatus and had a clear line of site to the testing area (Figure 6a). Setting up the RTS averaged 25 to 30 min to ensure everything was correct and ready to operate for each test. To collect data with the RTS unit, a team member held a survey rod with a prism on a particular point (Figure 6b), made sure of the plumpness of the rod, and then recorded the point data into a handheld data collector. This was done in a very meticulous manner to capture as many elevation changes as possible. To collect data without disturbing the surface, a piece of lumber was used as a bridge for the team member to get the measurements (Figure 6b).

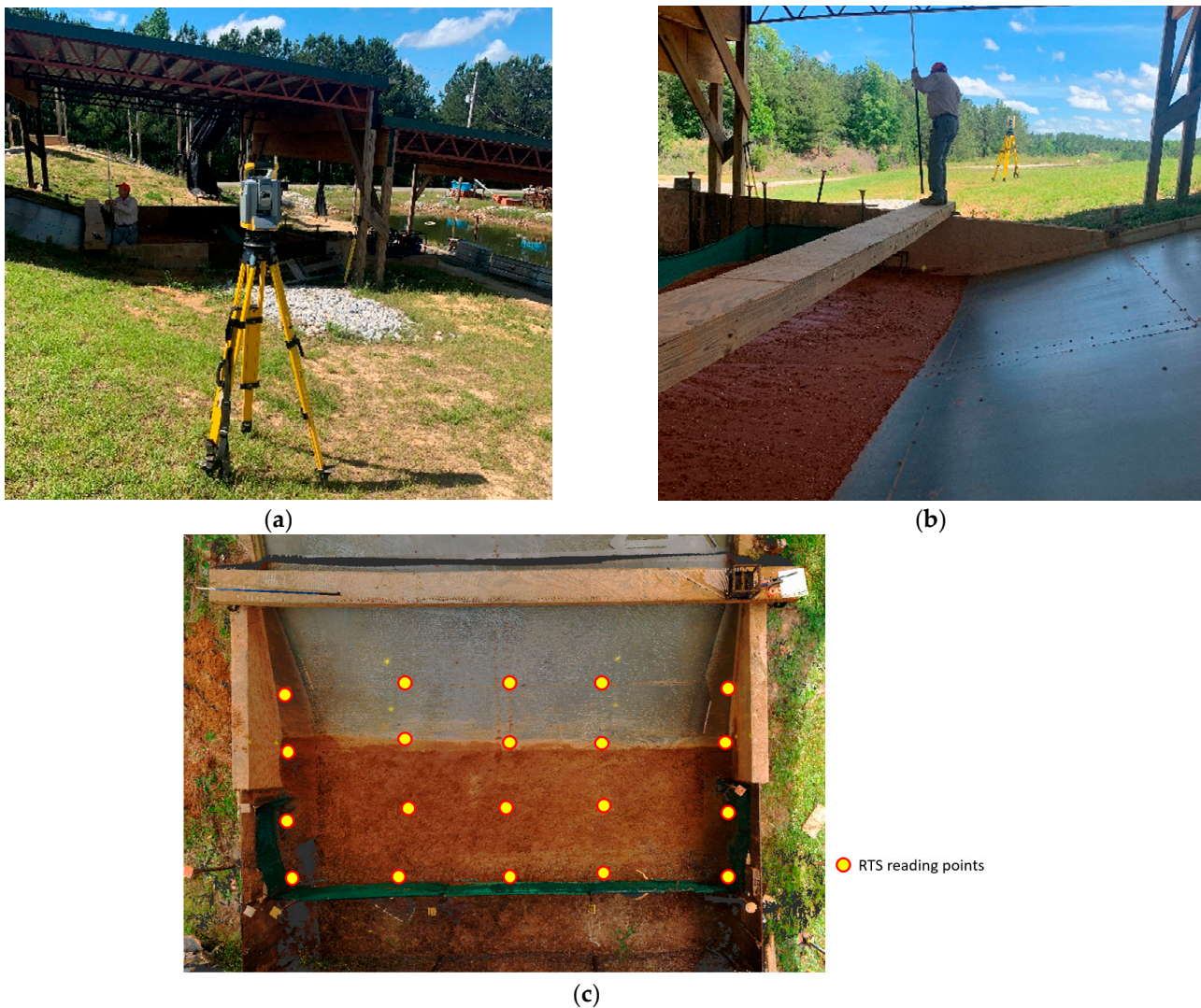


**Figure 6.** Using a RTS to capture elevations of the surface of the sediment retention area: (a) A Trimble SPS610 5'' RTS was set up next to the testing apparatus; (b) A team member used a survey rod to take measurements of the sediment retention surface from a piece of lumber that served as a bridge; (c) Locations of the 20 points captured by the RTS before Test#1.

The RTS unit was first used to record the surface of the testing area in the apparatus before Test#1. With the area being level and clean, it was determined only to capture twenty points. Of these twenty points (Figure 6c), five were taken across the slope approximately two feet (0.61 m) up, five were taken laterally across the bottom, and the remaining ten were taken in the flat test area. This was the base topography on which all the other tests were built. Then, 24 h after each test was run, the RTS was set up again and used to record points evenly distributed on the sediment buildup of that test run. The time spent to record points after each test was between 45–60 min on top of the 25–30 min required to set up the total station.

## 4. Results and Discussion

### 4.1. Data Processing

#### 4.1.1. TLS Scans

The “raw” scans captured by the FARO S-350 were transferred to a PC using a Secure Digital (SD) memory card before being processed in FARO SCENE software [36]. Each set of scans was processed individually for colorization, registration, and fusion into one point cloud. Registration errors occur when combining multiple 3D laser scans to form a

single point cloud, which is used to quantify the quality of merging multiple scans. They result from misalignments, inaccurate reference points, or scanner calibration issues. One common method to calculate the registration error is to use the Root Mean Square Error (RMSE) (Equation (1)):

$$RMSE = \sqrt{\frac{\sum d_i^2}{N}} \tag{1}$$

where  $d_i$  is the distance between a pair of corresponding points, and  $N$  is the total number of pairs considered. The registration results of all four sets of TLS scans (shown in Table 1) are relatively low, indicating good registration quality with sufficient overlap between scans of each test. Next, each point cloud was exported from FARO SCENE as an unordered RCP file. Then this RCP file was retrieved in Autodesk ReCap Pro (or ReCap) software [37] for cleaning and trimming. After this last step in ReCap, a high-density 3D colored point cloud representing the spatial information of the surface of the testing area has been created. Figure 7 illustrates the results of the TLS scan processing, including a comparison of “raw” and “cleaned” point clouds for each testing area. The “raw” point clouds show initial TLS data, while the “cleaned” point clouds result from data processing and filtering to remove noise and irrelevant data points. The comparison highlights the effectiveness of the processing techniques, yielding a clearer and more accurate representation of the testing surfaces for sediment retention analysis.

**Table 1.** TLS scan registration results.

TLS Scan Set	Mean Point Error	Max. Point Error	Min. Overlap
Before Test#1 run	0.9 mm	1.2 mm	71.1%
After Test#1 run	0.8 mm	1.0 mm	73.2%
After Test#2 run	0.7 mm	0.9 mm	74.1%
After Test#3 run	0.8 mm	1.0 mm	73.3%

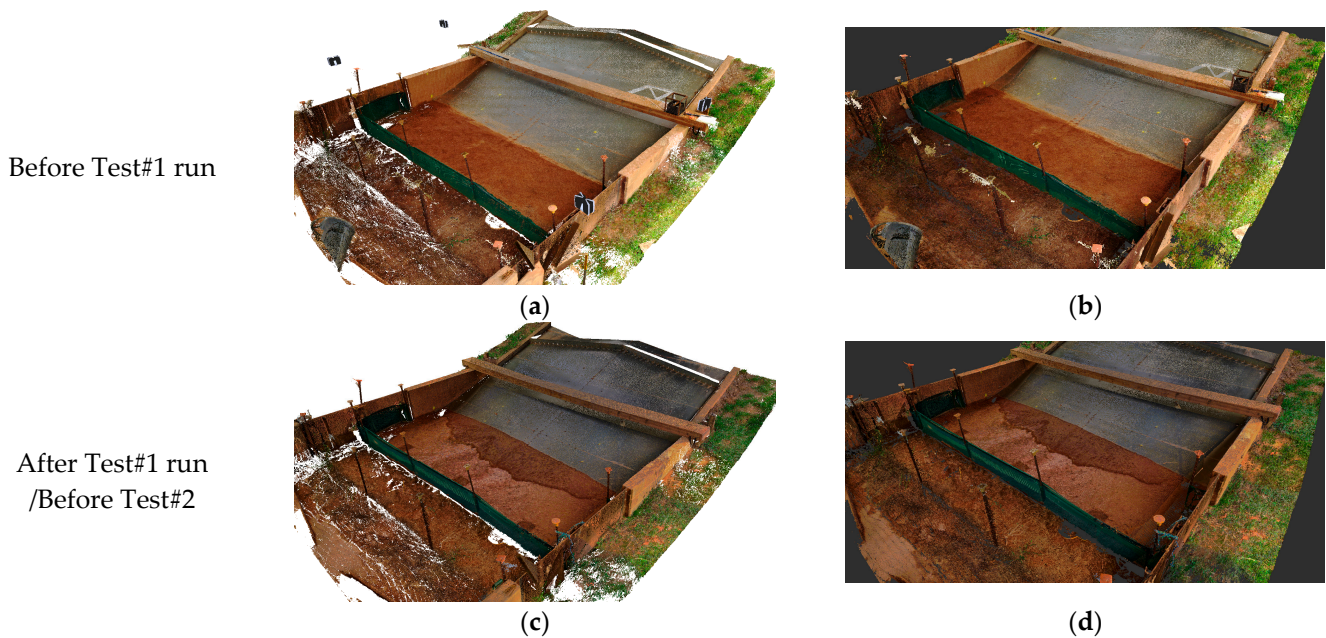


**Figure 7.** Cont.

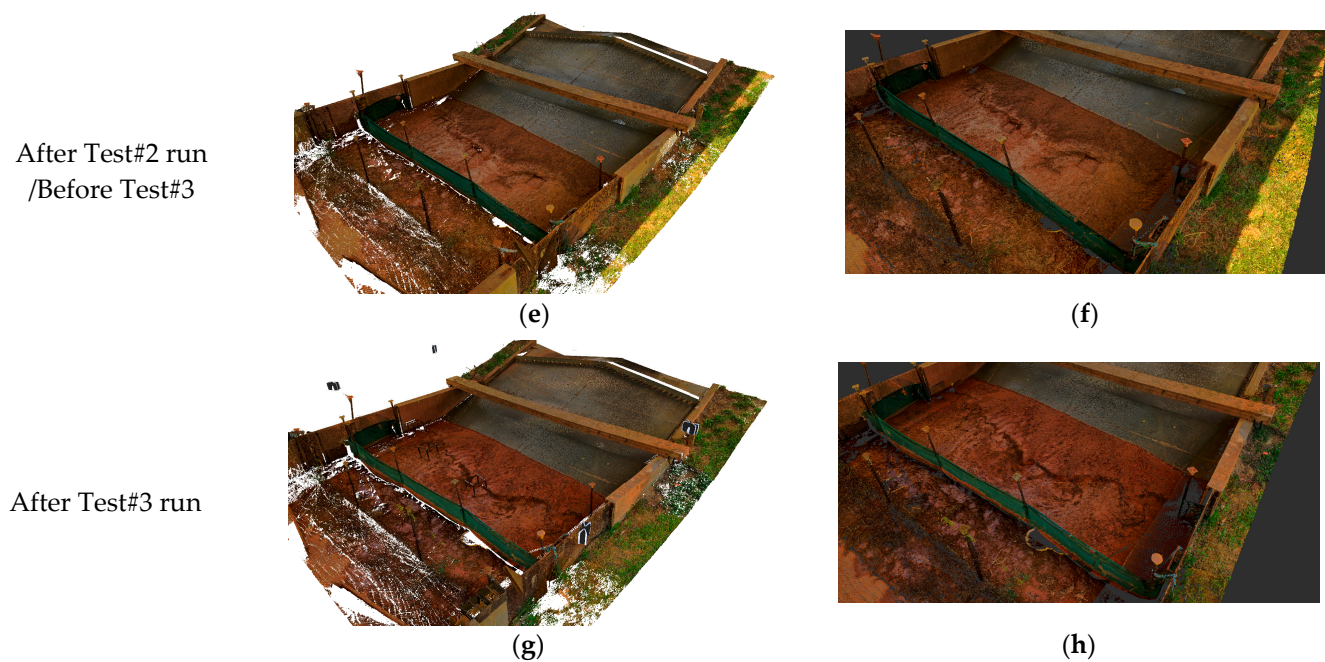


**Figure 7.** Results of the four processed TLS point clouds. (a) Registered point cloud in FARO SCENE. (b) Cleaned point cloud in ReCap. (c) Registered point cloud in FARO SCENE. (d) Cleaned point cloud in ReCap. (e) Registered point cloud in FARO SCENE. (f) Cleaned point cloud in ReCap. (g) Registered point cloud in FARO SCENE. (h) Cleaned point cloud in ReCap.

#### 4.1.2. RTS Points

The data of the points recorded by RTS surveys were downloaded from the data collector and then processed and stored in a Microsoft Excel document. This Excel file contained information on each captured point, including its unique label, Easting coordinate, Northing coordinate, and elevation. Table 2 shows the number of points captured for each test and their allocation on the surface of the testing area.

#### 4.2. Results

An equation (Equation (2)) was used to calculate the volumetric quantity of the sediment accumulated in the testing area of each test.

$$\Delta V_i = V_i - V_{i-1} \quad (2)$$

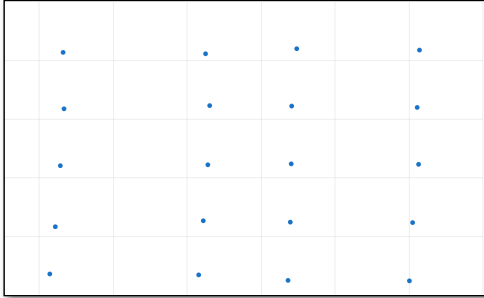
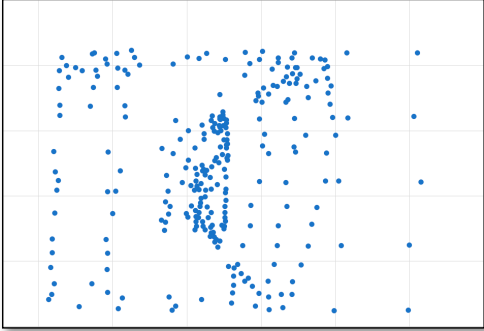
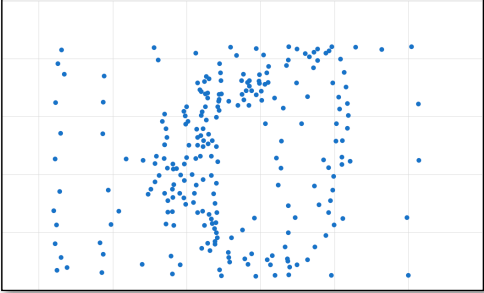
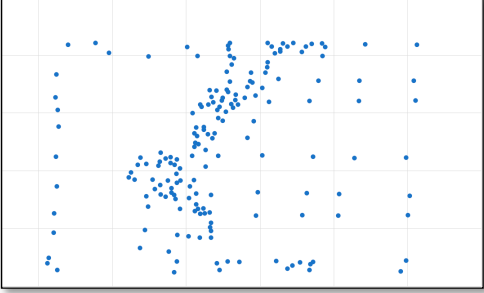
where  $\Delta V_i$  is the volume of the sediment deposit created from a test run,  $V_i$  is the volume of the soil in the testing area measured after this test run, and  $V_{i-1}$  is the volume of the soil in the testing area measured after the previous test run and before this test.

The data captured from TLS and RTS surveys were imported to Autodesk Revit to create Digital Elevation Models (DEMs) to determine volumetric differences in sediment deposits upstream of the SB system.

##### 4.2.1. Developing DEMs in Revit

All four TLS point clouds in the RCP file format were linked to a model in Revit. Figure 8 is an elevation view of the four-point clouds stacked on each other, showing the accumulation of soil sediment in the testing area after each run and conceptualising the TLS measurements' accuracy. Next, a highly detailed DEM for the testing area (as shown in Figure 9) was generated from the point cloud data using a specific command in the FARO As-Built for Autodesk Revit add-on (As-Built for Revit) [38].

**Table 2.** Points recorded by the RTS on the surface of the sediment retention of each test.

RTS Capture Stage	Number of Points	Scatter Chart of Captured Points
Before Test#1 run	20	
After Test#1 run	271	
After Test#2 run	243	<p data-bbox="1203 1059 1251 1088" style="text-align: center;">2.55</p> 
After Test#3 run	178	

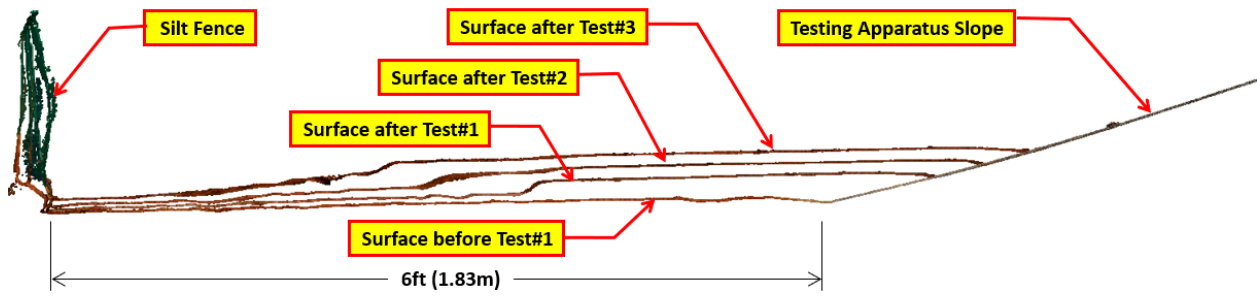


Figure 8. An elevation view of all four TLS point clouds stacked together showing the accumulation of soil sediment in the testing area after each test run.

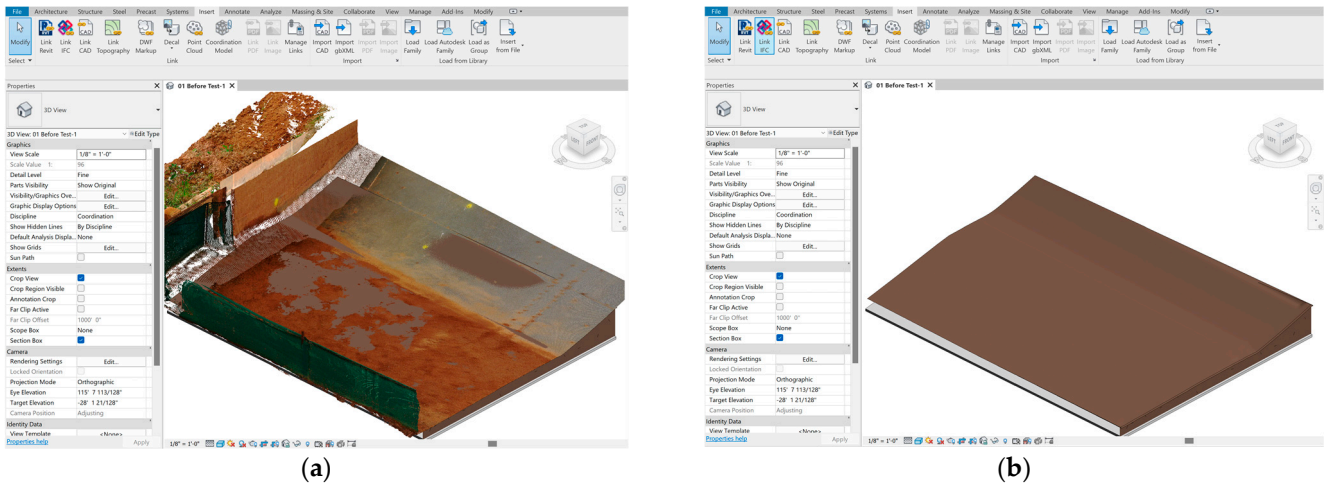


Figure 9. The process of creating a DEM of the testing area from a TLS point cloud in Revit: (a) A point cloud linked to a Revit model; (b) A DEM of the testing area created in Revit.

Revit enables the generation of topographical surfaces by importing point data files. By utilizing this capability with the RTS point data files, four additional DEMs were generated within the software. Figure 10 illustrates an example of a DEM created in Revit using the RTS data.

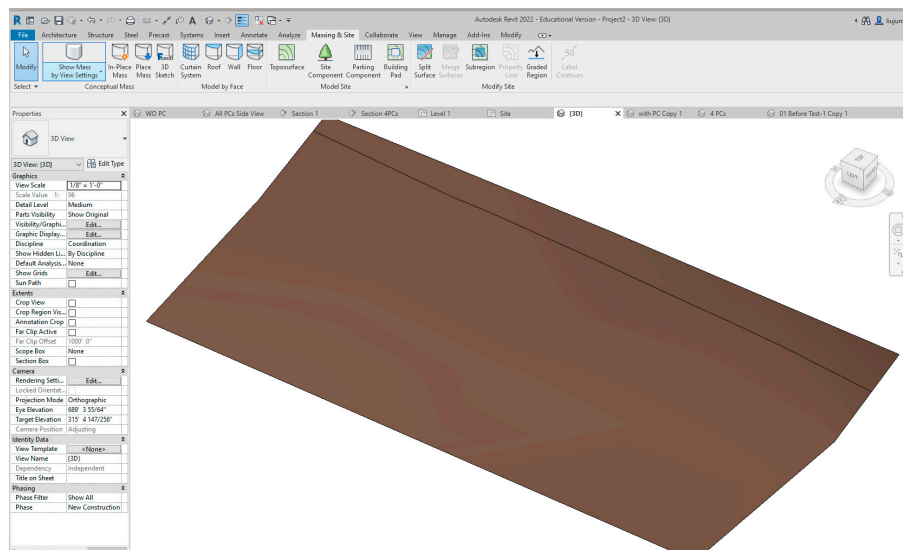


Figure 10. A DEM of the surface of the testing area before Test#1 was created using the RTS survey data in Revit.

#### 4.2.2. Using DEMs to Quantify Sediment Retention

Revit has a feature to compare two topographies and create “cut-and-fill” values to show their volumetric differences. Utilizing this feature, the volume ( $V_{\Delta}$ ) of the sediment retention (SR) of SD created from a test run is calculated using the initial and final DEMs of the test. Figure 11 presents a visual comparison between initial and final sediment deposition patterns and volume changes for each test run, utilizing DEMs generated from both TLS and RTS datasets. This illustration effectively highlights the differences in sediment accumulation and volume shifts observed throughout the experiment. Table 3 presents the results of the two sets of SR volumes calculated using the cut-and-fill function in Revit.

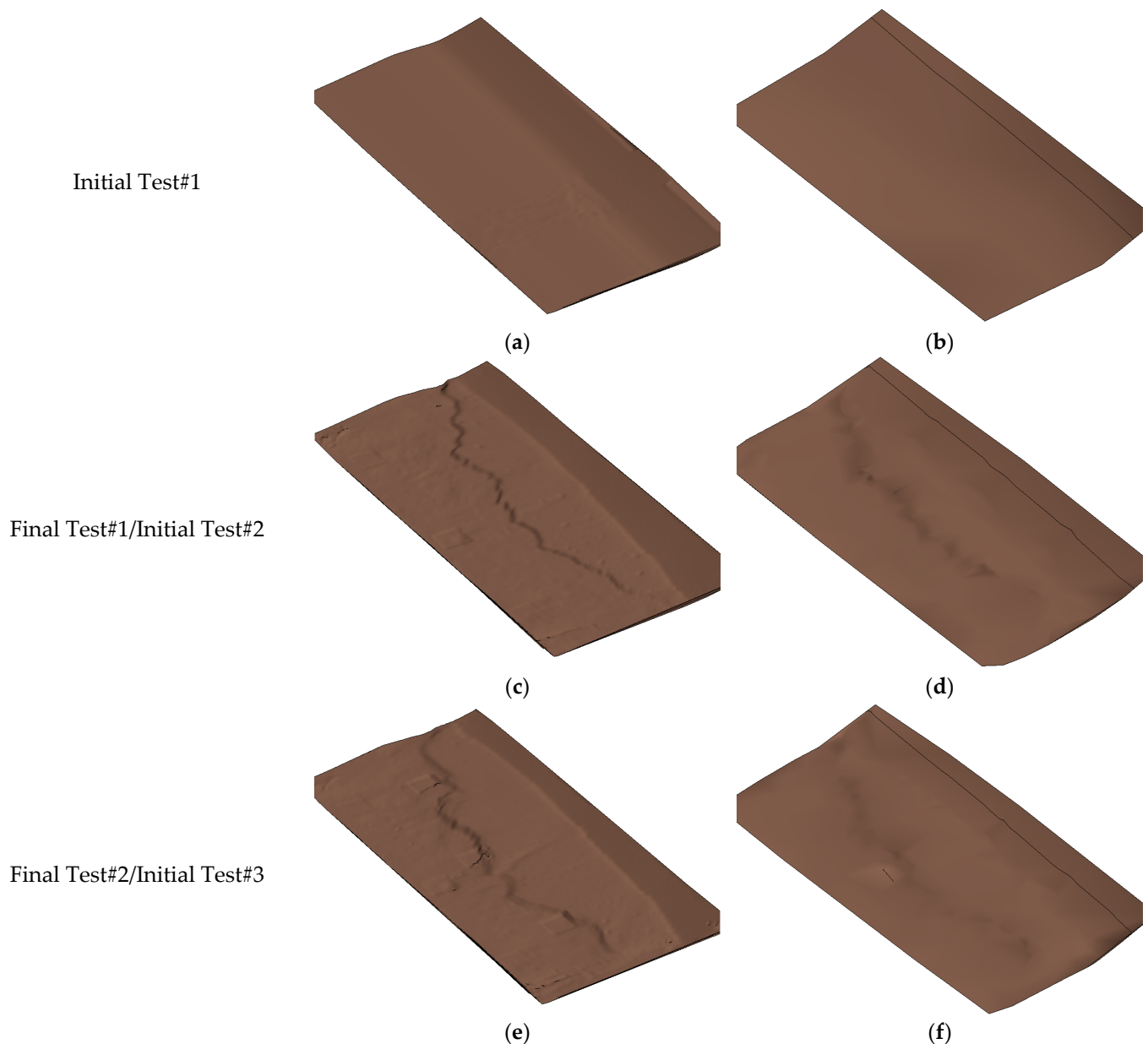
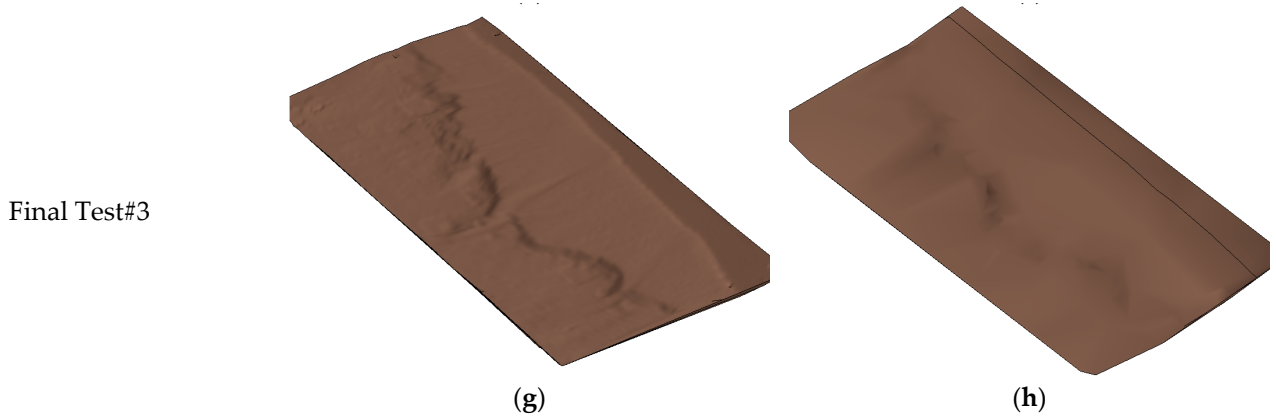


Figure 11. Cont.



**Figure 11.** Visual comparison of initial and final sediment deposition patterns and volume changes using DEMs from TLS and RTS datasets for each test run. (a) TLS DEM. (b) RTS DEM. (c) TLS DEM. (d) RTS DEM. (e) TLS DEM. (f) RTS DEM. (g) TLS DEM. (h) RTS DEM.

**Table 3.** The volumes of sediment retention of each test measured using two methods.

	SR Vol. Calculated from TLS DEMs			SR Vol. Calculated from RTS DEMs		
	Net Cut/Fill	Fill	Cut	Net Cut/Fill	Fill	Cut
Test#1	10.16 cf (0.288 m <sup>3</sup> )	10.60 cf (0.300 m <sup>3</sup> )	0.44 cf (0.012 m <sup>3</sup> )	13.61 cf (0.386 m <sup>3</sup> )	13.91 cf (0.394 m <sup>3</sup> )	0.30 cf (0.008 m <sup>3</sup> )
Test#2	9.26 cf (0.262 m <sup>3</sup> )	9.32 cf (0.264 m <sup>3</sup> )	0.06 cf (0.002 m <sup>3</sup> )	8.84 cf (0.250 m <sup>3</sup> )	9.48 cf (0.268 m <sup>3</sup> )	0.64 cf (0.018 m <sup>3</sup> )
Test#3	10.14 cf (0.287 m <sup>3</sup> )	10.18 cf (0.288 m <sup>3</sup> )	0.04 cf (0.001 m <sup>3</sup> )	11.18 cf (0.317 m <sup>3</sup> )	11.75 cf (0.333 m <sup>3</sup> )	0.57 cf (0.016 m <sup>3</sup> )

4.3. Discussion

Using a graph to compare the results between the two measurement methods, as seen in Figure 12, it appears that the TLS results are more linear than the RTS results indicating a higher correlation between the TLS results.

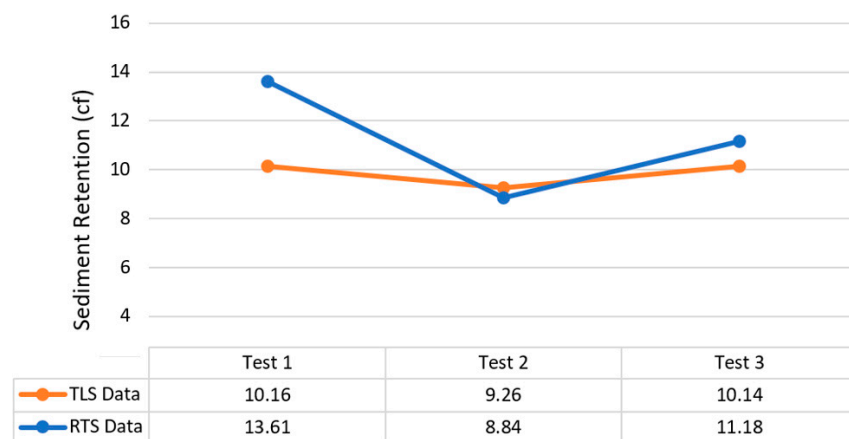


**Figure 12.** A correlation chart to compare the results between the two measurement methods.

To further analyze the results from the two measurement methods, the variance formula (Equation (3)) was introduced to identify a variance which helped find the standard deviation of the data for both TLS and RTS surveys.

$$\sigma^2 = \sum_{i=1}^N (x_i - \mu)^2 / N \tag{3}$$

The results are as follows:

TLS  $\sigma^2$  (variance) = 0.17  $\sigma$  (standard deviation) = 0.41 ft<sup>3</sup>

RTS  $\sigma^2$  (variance) = 3.77  $\sigma$  (standard deviation) = 1.94 ft<sup>3</sup>

Calculating the standard deviation from the variance formula provided a valuable measure of dispersion in the data, enabling the generation of a normal curve (bell curve) diagram in conjunction with the mean ( $\mu$ ). A narrow curve indicates the TLS data is more consistent as it is closer to the mean ( $\mu$ ), whereas a wider curve indicates the RTS data is farther from the mean ( $\mu$ ) and less consistent (see Figure 13). These statistics indicate that TLS is more accurate in measuring sediment retention than RTS surveys.

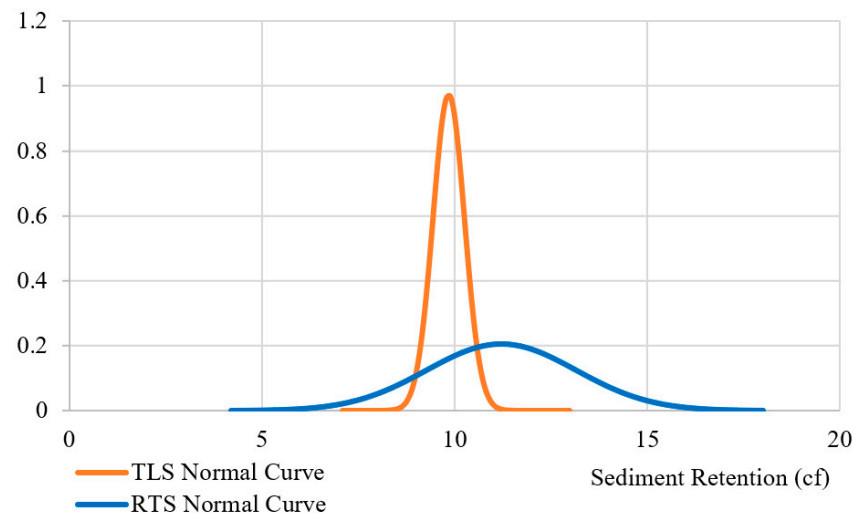


**Figure 13.** Bell curves for the measurement results of both TLS and RTS methods.

While conducting the data collection using TLS and RTS, the time and effort to perform the testing were observed. The TLS method took four scans in approximately one hour for each test, including scanner set-up and scanning. In addition, TLS was a more automated process requiring one person to perform scanning and allowing them to be hands-free while the scanner was running. Also, the high-density colorized 3D point clouds produced from TLS gave a detailed, accurate, comprehensive, and concise visual representation of the surface area for each test.

On the other hand, hundreds of points were recorded manually when using the RTS to survey the surface of the testing area after a test run. This process for each test took about 70–90 min to complete but failed to provide results as detailed as TLS. The manual nature of the RTS method introduces variability in point density and distribution (as shown in Table 2) due to factors such as operator judgment, accessibility, and visibility of the testing surface. Despite efforts to maintain consistency, some variation in point density is inevitable with RTS, highlighting its inconsistency compared to the more uniform point cloud generation provided by TLS. For the RTS to produce results comparable to the TLS results, every square inch of the testing area would have to be recorded, with the size of the testing area being 20 ft.  $\times$  6 ft. (6.1 m  $\times$  1.8 m) would be around 17,000 points to record. Human factors involved in conducting point recordings, such as holding a survey rod to just touch the top of the soil surface and maintaining eye level, make it a time-consuming and challenging task with a significant margin for error, as shown in Figure 14a. Achieving consistency over thousands of recordings would be next to impossible. Figure 14b illustrates the challenges and inaccuracies of this method as the rod's dimples on the soil surface distort the surface, negatively affecting the final data.

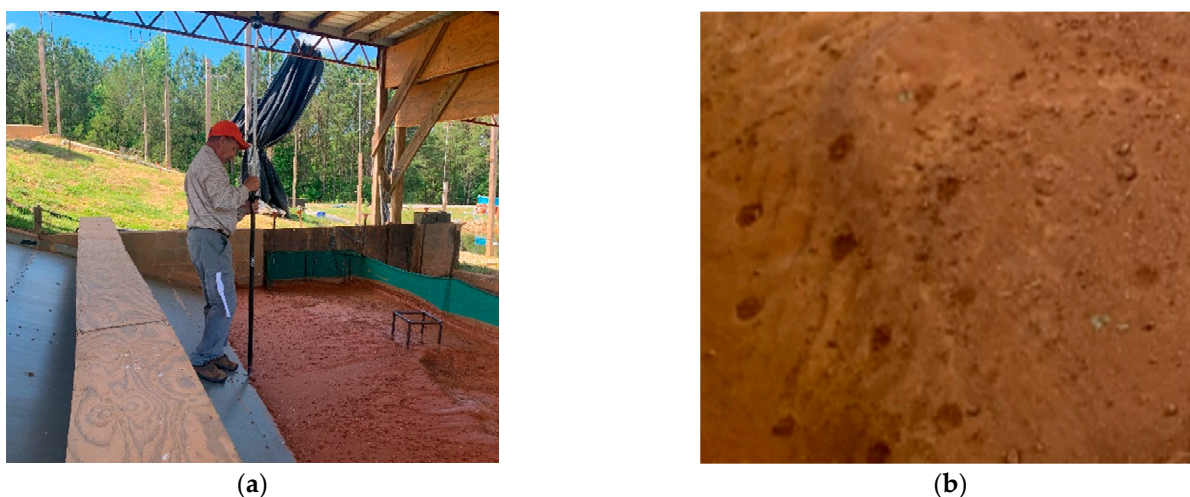


**Figure 14.** Challenges of using RTS to capture the surface: (a) A team member was holding the survey rod plumb; (b) “Dimples” on the soil surface created by the rod.

### 5. Conclusions and Recommendations for Future Research

Studying sediment barriers (SBs) through experimental testing is an effective way to understand the limitations and capacity of these barriers. This research investigates the effectiveness of Terrestrial Laser Scanning (TLS) and Robotic Total Station (RTS) techniques in quantifying sediment retention during full-scale sediment barrier testing. The comparative analysis of these methods demonstrated that while TLS and RTS can measure sediment retention, TLS offers greater accuracy and effectiveness than RTS.

One of the primary advantages of TLS is its ability to capture a detailed and comprehensive representation of the testing area surface, accounting for all irregularities, textures, and variations. Additionally, the field operation of TLS is relatively simple and quick, yielding high-resolution point clouds that allow for more in-depth analysis. However, it is essential to consider that processing TLS scans requires proficiency in multiple software programs, which can be challenging for practitioners. Furthermore, the utilization of TLS demands expensive equipment, several specialty software programs, and highly trained professionals to perform the task effectively [39]. In contrast, the RTS method must capture thousands of points to achieve results comparable to those obtained through TLS, rendering the process time-consuming, labor-intensive, and susceptible to errors. Although RTS may suffice when the primary goal is to identify general high and low spots of a surface without requiring fine detail, TLS remains a superior method for accurate measurement and comprehensive data analysis.

It is worth noting that TLS data collection is faster in the field compared to RTS. However, due to the registration process, TLS data processing and Digital Elevation Model (DEM) creation in Revit takes more time. Nevertheless, analyzing TLS data in a controlled office environment rather than in the field offers a comfort advantage over RTS, which may lead to a more accurate and efficient analysis.

Furthermore, human factors introduced during RTS data collection, such as holding the survey rod plumb and ensuring accurate contact with the soil surface, may result in a higher error margin than the more automated TLS process. The visual nature of point recording with RTS may also introduce bias, as operators may unintentionally overlook certain areas, resulting in incomplete data capture.

In conclusion, this research validates the benefits of TLS for sediment deposit volume research and suggests its adoption as a potential new standard in sediment barrier testing. TLS provides more accurate and detailed results and demonstrates greater efficiency and ease of use than RTS. However, it is crucial to recognize that the findings’ applicability to natural ground conditions may be affected by factors such as soil type, vegetation, and topography.

For future research, it is recommended to explore modifications to testing apparatus configurations to improve the accuracy and relevance of the results. Conducting further tests with different sediment barrier types can also provide valuable insights into the performance of these systems under varying conditions. Implementing changes that promote a more even sediment distribution in the testing area can enhance consistency and accuracy in the results, ultimately contributing to a more comprehensive understanding of sediment barrier performance and informing the development of improved sediment control strategies.

**Author Contributions:** Conceptualization, J.L., R.A.B. and C.W.F.; methodology, J.L., R.A.B. and C.W.F.; validation, J.L. and C.W.F.; formal analysis, J.L. and C.W.F.; investigation, J.L. and C.W.F.; data curation, J.L. and C.W.F.; writing, J.L.; visualization, J.L. and C.W.F. All authors have read and agreed to the published version of the manuscript.

**Funding:** This research received no external funding.

**Institutional Review Board Statement:** Not Applicable.

**Informed Consent Statement:** Not Applicable.

**Data Availability Statement:** The data that support the findings of this study are available upon request from the corresponding author. Due to the sensitive nature of the data and their file size, access to the data will be granted on a case-by-case basis and may require a data use agreement to be signed.

**Conflicts of Interest:** The authors declare no conflict of interest.

## References

1. Toy, T.J.; Foster, G.R.; Renard, K.G. *Soil Erosion: Processes, Prediction, Measurement, and Control*; John Wiley & Sons: Hoboken, NJ, USA, 2002; ISBN 978-0-471-38369-7.
2. Bugg, R.A.; Donald, W.; Zech, W.; Perez, M. Performance Evaluations of Three Silt Fence Practices Using a Full-Scale Testing Apparatus. *Water* **2017**, *9*, 502. [CrossRef]
3. Whitman, J.B.; Zech, W.C.; Donald, W.N. Full-Scale Performance Evaluations of Innovative and Manufactured Sediment Barrier Practices. *Transp. Res. Rec. J. Transp. Res. Board* **2019**, *2673*, 284–297. [CrossRef]
4. Barrett, M.E.; Malina, J.F.; Charbeneau, R.J. An Evaluation of Geotextiles for Temporary Sediment Control. *Water Environ. Res.* **1998**, *70*, 283–290. [CrossRef]
5. Whitman, J.B.; Zech, W.C.; Donald, W.N.; LaMondia, J.J. Full-Scale Performance Evaluations of Various Wire-Backed Nonwoven Silt Fence Installation Configurations. *Transp. Res. Rec.* **2018**, *2672*, 68–78. [CrossRef]
6. Rhea, D. Roadside Guide to Clean Water: Sediment Barriers. Available online: <https://extension.psu.edu/roadside-guide-to-clean-water-sediment-barriers> (accessed on 15 December 2022).
7. Whitman, J.B.; Zech, W.C.; Donald, W.N. Improvements in Small-Scale Standardized Testing of Geotextiles Used in Silt Fence Applications. *Geotext. Geomembr.* **2019**, *47*, 598–609. [CrossRef]
8. Perez, M.A.; Zech, W.C.; Donald, W.N.; Turochy, R.; Fagan, B.G. Transferring Innovative Erosion and Sediment Control Research Results into Industry Practice. *Water* **2019**, *11*, 2549. [CrossRef]
9. Yakar, M. Digital Elevation Model Generation by Robotic Total Station Instrument. *Exp. Technol.* **2009**, *33*, 52–59. [CrossRef]
10. Landphair, H.; McFalls, J.; Peterson, B.; Li, M. Alternatives to Silt Fence for Temporary Sediment Control at Highway Construction Sites: Guidelines for TxDOT. 1997. Available online: <https://www.semanticscholar.org/paper/Alternatives-to-Silt-Fence-for-Temporary-Sediment-Landphair-McFalls/d98246d48bfc6ad652d691099926929abd5cf060> (accessed on 15 December 2022).
11. DeMoranville, C.; Sandler, H. Erosion & Sediment Control BMP: Publications UMass Cranberry Station. Available online: [https://www.umass.edu/cranberry/pubs/bmp\\_erosion.html](https://www.umass.edu/cranberry/pubs/bmp_erosion.html) (accessed on 15 December 2022).
12. Whitman, J.B.; Perez, M.A.; Zech, W.C.; Donald, W.N. Practical Silt Fence Design Enhancements for Effective Dewatering and Stability. *J. Irrig. Drain. Eng.* **2021**, *147*, 04020039. [CrossRef]
13. Gogo-Abite, I.; Chopra, M. Performance Evaluation of Two Silt Fence Geotextiles Using a Tilting Test-Bed with Simulated Rainfall. *Geotext. Geomembr.* **2013**, *39*, 30–38. [CrossRef]
14. Keener, H.M.; Faucette, B.; Klingman, M.H. Flow-through Rates and Evaluation of Solids Separation of Compost Filter Socks versus Silt Fence in Sediment Control Applications. *J. Environ. Qual.* **2007**, *36*, 742–752. [CrossRef]
15. Zech, W.C.; Halverson, J.L.; Clement, T.P. Intermediate-Scale Experiments to Evaluate Silt Fence Designs to Control Sediment Discharge from Highway Construction Sites. *J. Hydrol. Eng.* **2008**, *13*, 497–504. [CrossRef]

16. Zimmie, T.F.; Kamalzare, M. Measuring the Rate of Sediment Transport and Erosion in Physical Model Testing. In Proceedings of the Innovations in Geotechnical Engineering, Orlando, FL, USA, 5–10 March 2018; American Society of Civil Engineers: Orlando, FL, USA, 2018; pp. 330–341.
17. Tran, T.V.; Tucker-Kulesza, S.E.; Bernhardt, M. Soil Surface Roughness and Turbidity Measurements in Erosion Testing. *IFCEE* **2018**, *2018*, 506–515. [[CrossRef](#)]
18. Keim, R.F.; Skaugset, A.E.; Bateman, D.S. Digital Terrain Modeling of Small Stream Channels with a Total-Station Theodolite. *Adv. Water Resour.* **1999**, *23*, 41–48. [[CrossRef](#)]
19. Eltner, A.; Baumgart, P. Accuracy Constraints of Terrestrial Lidar Data for Soil Erosion Measurement: Application to a Mediterranean Field Plot. *Geomorphology* **2015**, *245*, 243–254. [[CrossRef](#)]
20. Luffman, I.; Nandi, A.; Luffman, B. Comparison of Geometric and Volumetric Methods to a 3D Solid Model for Measurement of Gully Erosion and Sediment Yield. *Geosciences* **2018**, *8*, 86. [[CrossRef](#)]
21. Li, L.; Lan, H.; Peng, J. Loess Erosion Patterns on a Cut-Slope Revealed by LiDAR Scanning. *Eng. Geol.* **2020**, *268*, 105516. [[CrossRef](#)]
22. Resop, J.P.; Hession, W.C. Terrestrial Laser Scanning for Monitoring Streambank Retreat: Comparison with Traditional Surveying Techniques. *J. Hydraul. Eng.* **2010**, *136*, 794–798. [[CrossRef](#)]
23. Myers, D.T.; Rediske, R.R.; McNair, J.N. Measuring Streambank Erosion: A Comparison of Erosion Pins, Total Station, and Terrestrial Laser Scanner. *Water* **2019**, *11*, 1846. [[CrossRef](#)]
24. Danino, D.; Svoray, T.; Thompson, S.; Cohen, A.; Crompton, O.; Volk, E.; Argaman, E.; Levi, A.; Cohen, Y.; Narkis, K.; et al. Quantifying Shallow Overland Flow Patterns Under Laboratory Simulations Using Thermal and LiDAR Imagery. *Water Resour. Res.* **2021**, *57*, e2020WR028857. [[CrossRef](#)]
25. Victoriano, A.; Brasington, J.; Guinau, M.; Furdada, G.; Cabré, M.; Moysset, M. Geomorphic Impact and Assessment of Flexible Barriers Using Multi-Temporal LiDAR Data: The Portainé Mountain Catchment (Pyrenees). *Eng. Geol.* **2018**, *237*, 168–180. [[CrossRef](#)]
26. Heritage, G.; Hetherington, D. Towards a Protocol for Laser Scanning in Fluvial Geomorphology. *Earth Surf. Process Landf.* **2007**, *32*, 66–74. [[CrossRef](#)]
27. Li, H. Investigation of Highway Stormwater Management Pond Capacity for Flood Detention and Water Quality Treatment Retention via Remote Sensing Data and Conventional Topographic Survey. *Transp. Res. Rec.* **2020**, *2674*, 514–527. [[CrossRef](#)]
28. Valentini, E.; Taramelli, A.; Cappucci, S.; Filippini, F.; Nguyen Xuan, A. Exploring the Dunes: The Correlations between Vegetation Cover Pattern and Morphology for Sediment Retention Assessment Using Airborne Multisensor Acquisition. *Remote Sens.* **2020**, *12*, 1229. [[CrossRef](#)]
29. James, L.A.; Watson, D.G.; Hansen, W.F. Using LiDAR Data to Map Gullies and Headwater Streams under Forest Canopy: South Carolina, USA. *CATENA* **2007**, *71*, 132–144. [[CrossRef](#)]
30. Li, L.; Nearing, M.A.; Nichols, M.H.; Polyakov, V.O.; Cavanaugh, M.L. Using Terrestrial LiDAR to Measure Water Erosion on Stony Plots under Simulated Rainfall. *Earth Surf. Process Landf.* **2020**, *45*, 484–495. [[CrossRef](#)]
31. Bailey, G. Challenges in Approaching the Detection Limits for Hillslope Erosion Using Terrestrial Laser Scanning. Master’s Thesis, University of Tennessee, Knoxville, TN, USA, 2022.
32. Bugg, R.A.; Donald, W.N.; Zech, W.C.; Perez, M.A. Improvements in Standardized Testing for Evaluating Sediment Barrier Performance: Design of a Full-Scale Testing Apparatus. *J. Irrig. Drain. Eng.* **2017**, *143*, 04017029. [[CrossRef](#)]
33. FARO Focus Laser Scanner | FARO. Available online: <https://www.faro.com/en/Products/Hardware/Focus-Laser-Scanners> (accessed on 19 December 2022).
34. Trimble S5 | Robotic Total Stations | Trimble Geospatial. Available online: <https://geospatial.trimble.com/products-and-solutions/trimble-s5> (accessed on 16 December 2022).
35. Crumal, Z. What Is a Robotic Total Station? Here’s Everything You Need to Know. Available online: <https://bim360resources.autodesk.com/connect-construct/what-is-a-robotic-total-station-heres-everything-you-need-to-know> (accessed on 17 December 2022).
36. FARO@SCENE 3D Point Cloud Software | FARO. Available online: <https://www.faro.com/en/Products/Software/SCENE-Software> (accessed on 26 November 2022).
37. ReCap Software | What Is ReCap Pro? | Autodesk. Available online: <https://www.autodesk.com/products/recap/overview> (accessed on 26 November 2022).
38. Getting Started with As-Built for Autodesk Revit. Available online: [https://knowledge.faro.com/Software/As-Built/As-Built\\_for\\_Autodesk\\_Revit/Getting\\_Started\\_with\\_As-Built\\_for\\_Autodesk\\_Revit](https://knowledge.faro.com/Software/As-Built/As-Built_for_Autodesk_Revit/Getting_Started_with_As-Built_for_Autodesk_Revit) (accessed on 22 December 2022).
39. Palcak, M.; Kudela, P.; Fandakova, M.; Kordek, J. Utilization of 3D Digital Technologies in the Documentation of Cultural Heritage: A Case Study of the Kunerad Mansion (Slovakia). *Appl. Sci.* **2022**, *12*, 4376. [[CrossRef](#)]

**Disclaimer/Publisher’s Note:** The statements, opinions and data contained in all publications are solely those of the individual author(s) and contributor(s) and not of MDPI and/or the editor(s). MDPI and/or the editor(s) disclaim responsibility for any injury to people or property resulting from any ideas, methods, instructions or products referred to in the content.